research papers

Comparison of the structural motifs of aceto-acetanilides and related azo pigments

Greig Chisholm,[a]***** **Alan R. Kennedy,**[b] **Sharon Wilson**[a] **and Simon J. Teat**[c]

[a]Ciba Specialty Chemicals PLC, Hawkhead Road, Paisley PA2 7BG, Scotland, [b]Department of Pure and Applied Chemistry, University of Strathclyde, Glasgow G1 1XL, Scotland, and [c]CCLRC Daresbury Laboratory, Warrington WA4 4AD, England

Correspondence e-mail:
greig.chisholm@cibasc.com

The structures of three methyl-substituted acetoacetanilides and of an azo pigment derived from one of them are presented and discussed together with a review of related known crystal structures. By considering the position of any aromatic substituents it is possible to predict whether the simple acetoacetanilides adopt planar structures with intramolecular hydrogen bonding or twisted structures featuring intermolecular hydrogen bonding. However, we find that the same crystal engineering rules cannot be applied to the related azo pigments: this is apparently due to the presence of an sp^2 atom which facilitates the adoption of planar conformations. The thermal properties of the acetoacetanilides were measured by DSC and are discussed with reference to their crystal structures.

1. Introduction

Organic pigments find application in many areas, from the mass colouration of polymers and ink vehicles to the manufacture of electroluminescent devices. In order to understand the importance of the crystal structure of an organic pigment, one must appreciate the essential difference between a dye and a pigment. Simply put, a dye is at some stage soluble during its application, whereas a pigment remains as a crystalline solid throughout the application process. Given this crystalline nature, it is clear that the crystal structure of the pigment is of critical importance. Indeed, it determines properties such as the hue and the stability of the pigment to solvent, heat and light. Furthermore, the colour strength, hiding power, stability, flow and dispersion properties of a pigmentary material depend on the crystal morphology and the nature of the major surfaces of the crystal. These properties are again dependent on the crystal structure (Hao & Iqbal, 1997). Equally, in the broader context of crystal engineering, an understanding of the forces which cause molecules to aggregate in the solid state to give ordered and often enchanting patterns is important in the design of new materials and in our understanding of how molecules associate in solution.

The poor crystal growth properties of organic azo pigments, due to their inherent insolubility, makes routine structural analysis an extremely challenging problem. To date, only the β-naphthol (1) (Jarvis, 1961; Olivieri *et al.*, 1989; Salmen *et al.*, 1988; Whitaker, 1977, 1978*b*; Grainger & McConnell, 1969; Guggenberger & Teufer, 1975; Diamantis *et al.*, 1992; Alcock *et al.*, 1968), naphthol AS (2) (Kobelt *et al.*, 1972, 1974; Whitaker, 1978*a*) and acetoacetanilide (3) (Paulus *et al.*, 1983; Paulus, 1984; Gridunova *et al.*, 1991; Paulus & Rieper, 1985; Whitaker

1983*a,b*, 1984*a,b*, 1985*a,b,c*, 1986, 1987; Whitaker & Walker, 1987; Golinski, 1988) classes of pigment have given crystal structures using standard laboratory techniques. The difficulty

(1)

(2)

(3)

(4)

(5)

(6)

(7)

(8)

(9)

(10)

(11)

(12)
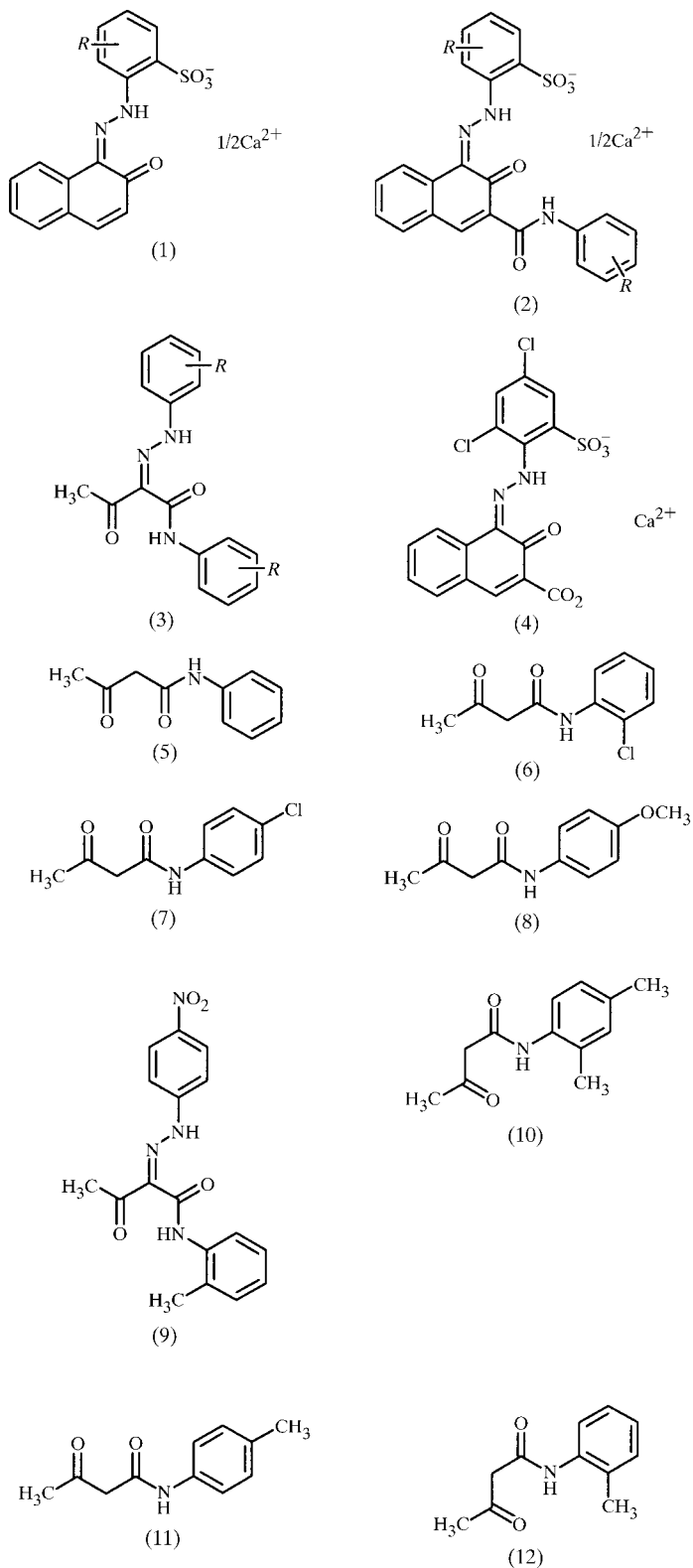
in growing good quality crystals is further shown by the poor quality of some of these determinations (*e.g.* Whitaker, 1977, 1978*a*). However, the recent wider availability of dedicated single-crystal stations at synchrotrons, such as Station 9.8 at Daresbury SRS (Cernik *et al.*, 1997), has allowed much smaller and more weakly diffracting crystals to be investigated. The first example of a naphthoic acid based pigment lake has recently been elucidated (4) (Kennedy *et al.*, 2000) using synchrotron radiation, as has the structure of an azo dye, rotaxane (Anderson *et al.*, 1998).
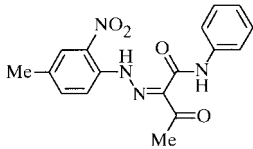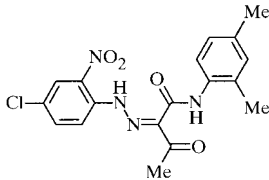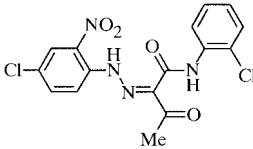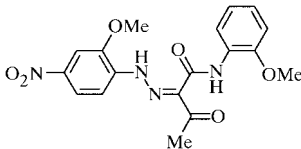
Acetoacetanilide (5) and related compounds are readily available, cheap and widely used as starting materials in the manufacture of organic pigments. These compounds are characterized by differences in the substitution of the aromatic ring which give rise to a range of organic pigments with differing properties (see Table 1 for examples). Pigments based on acetoacetanilide starting materials find application in a range of systems, including the colouration of inks, paints and plastics.

Typically during the synthesis of an organic azo pigment, the diazonium salt component is added to a slightly acidic aqueous slurry of the anilide. Despite the fact that the anilide exists at least partially as a crystalline material during synthesis, little is known about the crystal structures of these compounds. Kubozono *et al.* (1992) have reported the structures of (5), (6) and (7). The most recent publication in this area is by Bertolasi and co-workers (Bertolasi *et al.*, 1995) and represents the most detailed coverage of the topic to date: it discusses the N$\cdots$O distance for a range of compounds containing N—H$\cdots$O hydrogen bonds and in particular how the strength of these hydrogen bonds is assisted by resonance. Of particular relevance to our work is the anilide (8). Neither of these previous publications present the implications of this structural information in the context of pigment synthesis. The work presented in the current paper is a study of the crystal structures of several new compounds in this series, which are of relevance in their own right given the heterogeneous nature of pigment synthesis, but also seeks to further broaden our understanding of the packing forces prevalent in organic pigments. In addition we present the structure of the azo pigment (9) and discuss the relationship between the structure of the starting anilide and the final pigment.

2. Experimental

Acetoacet-*m*-xylidide (10), acetoacet-*p*-toluidide (11) and acetoacet-*o*-toluidide (12) were supplied by Lonza Chemicals. All other reagents were purchased from Aldrich Chemicals and were used without further purification. All aceto-acetanilides for crystal structure analysis were recrystallized from hot saturated solutions in acetone. After recrystallization each of the samples were passed through a 250 μm sieve and analysed by powder X-ray diffraction to determine whether any polymorphic change had taken place on recrystallization. Powder X-ray diffraction confirmed that each of the recrystallized samples belonged to the same crystal phase as the bulk material.

Table 1
Comparison of pigments derived from acetoacetanilides.

Pigment	Structure	Properties
Yellow 1		Mid-shade yellow High, light stability Poor solvent and heat stability
Yellow 2		Red-shade yellow Colour strength superior to Yellow 1, otherwise equivalent
Yellow 3		Green-shade yellow Very poor solvent stability, otherwise equivalent to Yellow 1
Yellow 74		Green-shade yellow Significantly higher colour strength and light stability than Yellow 1

was added and the mixture stirred for 30 min at 273 K before being filtered. The resultant diazonium salt solution was added over 15 min to a solution of acetoacet-*o*-toluidide (12) (1.9 g, 10 mmol) and sodium acetate (1.15 g) in methanol (25 ml) at 273 K. The slurry thus obtained was stirred for 1 h at 273 K before being allowed to warm to room temperature. The volume of the slurry was reduced to approximately half by evaporation on a rotary evaporator and allowed to stand overnight. The yellow crystals formed were isolated by filtration. The product was purified by recrystallization from toluene to give bright yellow micro-crystals (2.7 g, 67%).

Melting points and heats of fusion were determined on a TA4000 calorimeter over the temperature range 303–422 K and at a scan rate of 5 K min^{-1}. Powder X-ray diffraction patterns were recorded on a Siemens D5000 X-ray diffractometer in reflection mode using filtered Cu $K\alpha_1$ radiation. The total range in 2θ was 3–35°, measured in 0.02° steps and collected over 27 min.

2.1. Synthesis of *N*-(2-methyl)phenyl-2-(4-nitrophenylhydrazono)-3-oxobutyramide (9)

4-Nitroaniline (1.4 g, 10 mmol) was dissolved in a mixture of 36% hydrochloric acid (10 ml) and water (10 ml). The
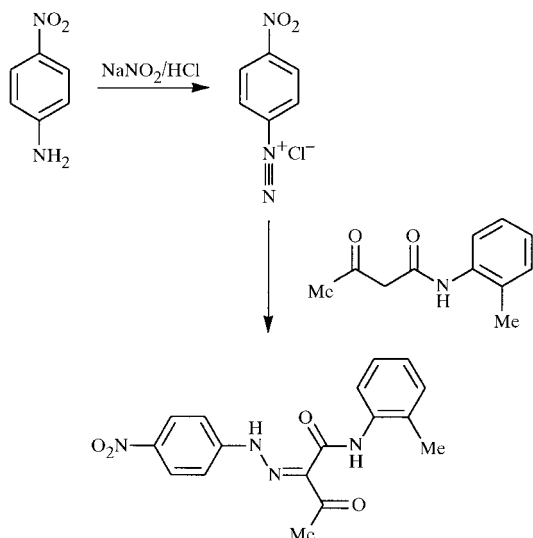
solution was cooled to 273 K by immersion in an ice bath. A solution of sodium nitrite (0.69 g, 10 mmol) in water (10 ml)

2.2. Single-crystal structure determinations

Measurements on (10), (11) and (12) were made at 123 K with a Rigaku AFC7*S* four-circle diffractometer and Mo $K\alpha$ radiation, $\lambda = 0.71069$ Å, using $\omega/2\theta$ scans. Measurements on (9) were made at 150 K using Si(111) monochromated synchrotron radiation, $\lambda = 0.6891$ Å, and a Siemens SMART CCD area-detector diffractometer using standard procedures and programs for Station 9.8 (Clegg *et al.*, 1998). The intensity decay of 35% includes a correction applied for synchrotron beam decay as well as for crystal decay correction. All structures were solved by direct methods and refined to convergence against F^2 using all unique reflections (*SHELX*; Sheldrick, 1997). Non-H atoms were treated anisotropically. In (11) and (12) H atoms were refined isotropically, except for the disordered methyl group of (11) where hydrogen positions were idealized. In (9) and (10) all H atoms were placed in calculated positions and in a riding mode. All H atoms were, however, observed in difference Fourier syntheses. Crystal data and experimental parameters are detailed in Table 2[1].

---

[1] Supplementary data for this paper are available from the IUCr electronic archives (Reference: BM0031). Services for accessing these data are described at the back of the journal.

Table 2
Experimental details.

Atomic scattering factors were taken from *International Tables for Crystallography* (1992, Vol. C, Tables 4.2.6.8 and 6.1.1.4). Programs used: for data collection *SMART* (Siemens, 1995) for (9) and MSC/Rigaku software (Molecular Structure Corporation, 1985) for (10), (11) and (12); for cell refinement: local program for (9) and MSC/Rigaku software (Molecular Structure Corporation, 1985) for (10), (11) and (12); for data reduction *SAINT* (Siemens, 1995) for (9) and *TEXSAN* (Molecular Structure Corporation, 1993) for (10), (11) and (12); for structure solution: *SHELXS* (Sheldrick, 1990); for structure refinement: *SHELXL*97 (Sheldrick, 1997).

	(9)	(10)	(11)	(12)
Crystal data				
Chemical formula	$C_{17}H_{16}N_4O_4$	$C_{12}H_{15}NO_2$	$C_{11}H_{13}NO_2$	$C_{11}H_{13}NO_2$
Chemical formula weight	340.34	205.25	191.22	191.22
Cell setting	Monoclinic	Monoclinic	Orthorhombic	Monoclinic
Space group	$P2_1/n$	$P2_1/m$	$Pbca$	$P2_1/c$
a (Å)	14.111 (6)	8.8636 (15)	26.766 (5)	7.3247 (10)
b (Å)	7.567 (3)	6.605 (3)	9.3754 (18)	12.108 (2)
c (Å)	15.338 (6)	9.2381 (17)	8.1729 (13)	10.7479 (14)
β (°)	99.967 (10)	97.804 (14)	90	99.357 (13)
V (Å^3)	1613.0 (11)	535.9 (3)	2050.9 (6)	940.5 (2)
Z	4	2	8	4
D_x (Mg m^{-3})	1.401	1.272	1.239	1.350
Radiation type	Synchrotron	Mo $K\alpha$	Mo $K\alpha$	Mo $K\alpha$
Wavelength (Å)	0.6891	0.71069	0.71069	0.71069
No. of reflections for cell parameters	5749	25	19	24
θ range (°)	2.5–23	16.94–17.93	6.62–9.11	10.10–17.74
μ (mm^{-1})	0.103	0.087	0.086	0.093
Temperature (K)	150 (2)	123 (2)	123 (2)	123 (2)
Crystal form	Plate	Cut needle	Plate	Needle
Crystal size (mm)	0.20 × 0.040 × 0.015	0.70 × 0.35 × 0.20	0.70 × 0.40 × 0.15	0.55 × 0.15 × 0.10
Crystal colour	Light yellow	Colourless	Colourless	Colourless
Data collection				
Diffractometer	Bruker SMART CCD	Rigaku AFC-7S	Rigaku AFC-7S	Rigaku AFC-7S
Data collection method	ω rotation with narrow frames	$\omega/2\theta$ scans	$\omega/2\theta$ scans	$\omega/2\theta$ scans
Absorption correction	Empirical	None	None	None
$T_{\min}$	0.9798	–	–	–
$T_{\max}$	0.9985	–	–	–
No. of measured reflections	5749	2714	4726	2104
No. of independent reflections	2445	1279	2363	1951
No. of observed reflections	1600	1031	1401	1168
Criterion for observed reflections	$I > 2\sigma(I)$	$I > 2\sigma(I)$	$I > 2\sigma(I)$	$I > 2\sigma(I)$
R_{int}	0.0689	0.0227	0.0392	0.0273
$\theta_{\max}$ (°)	23.00	27.00	27.50	26.51
Range of h, k, l	$-16 \rightarrow h \rightarrow 15$	$-11 \rightarrow h \rightarrow 11$	$-34 \rightarrow h \rightarrow 34$	$0 \rightarrow h \rightarrow 9$
	$-8 \rightarrow k \rightarrow 8$	$-8 \rightarrow k \rightarrow 8$	$-12 \rightarrow k \rightarrow 12$	$0 \rightarrow k \rightarrow 15$
	$-11 \rightarrow l \rightarrow 17$	$-11 \rightarrow l \rightarrow 11$	$-10 \rightarrow l \rightarrow 10$	$-13 \rightarrow l \rightarrow 13$
No. of standard reflections	–	3	3	3
Frequency of standard reflections	–	Every 150 reflections	Every 150 reflections	Every 150 reflections
Intensity decay (%)	–	0	0	0
Refinement				
Refinement on	F^2	F^2	F^2	F^2
$R[F^2>2\sigma(F^2)]$	0.0659	0.0333	0.0349	0.0428
$wR(F^2)$	0.1663	0.0985	0.1026	0.1280
S	0.998	1.066	0.986	1.072
No. of reflections used in refinement	2445	1279	2363	1951
No. of parameters used	231	94	168	180
H-atom treatment	Riding	Riding	All parameters refined	All parameters refined
Weighting scheme	$w = 1/[\sigma^2(F_o^2) + (0.096P)^2]$, where $P = (F_o^2 + 2F_c^2)/3$	$w = 1/[\sigma^2(F_o^2) + (0.041P)^2 + 0.162P]$, where $P = (F_o^2 + 2F_c^2)/3$	$w = 1/[\sigma^2(F_o^2) + (0.048P)^2 + 0.096P]$, where $P = (F_o^2 + 2F_c^2)/3$	$w = 1/[\sigma^2(F_o^2) + (0.043P)^2 + 0.269P]$, where $P =(F_o^2 + 2F_c^2)/3$
$(\Delta/\sigma)_{\max}$	0.001	< 0.001	0.040	< 0.001
$\Delta\rho_{\max}$ (e Å^{-3})	0.342	0.302	0.182	0.219
$\Delta\rho_{\min}$ (e Å^{-3})	−0.279	−0.219	−0.203	−0.199
Extinction method	*SHELXL*	*SHELXL*	None	*SHELXL*
Extinction coefficient	0.068 (9)	0.027 (5)	None	0.0070 (18)

Table 3
Hydrogen-bond distances (Å) and angles (°).

Molecule	N—H	H···O	N···O	N—H···O	Hydrogen-bond type
Acetoacetanilide (1)	0.92	2.00	2.909	172.9	Inter
Acetoaceto-o-chloroanilide (6)	0.90	1.92	2.708	144.6	Intra
Acetoaceto-p-chloroanilide (7)	0.82	2.09	2.874	161.0	Inter
Acetoacet-p-anisidide (8)	0.82	2.10	2.874	157.2	Inter
Azo pigment (9)	0.88	1.91	2.661 (4)	142.7	Intra
Acetoacet-m-xylidide (10)	0.88	1.96	2.712 (2)	142.4	Intra
Acetoacet-p-toluidide (11)	0.87 (2)	2.11 (2)	2.910 (2)	153 (1)	Inter
Acetoacet-o-toluidide (12)	0.87 (3)	1.92 (3)	2.704 (3)	149 (1)	Intra

† Symmetry code for acceptor O atom of (11) is $\frac{1}{2} - x, \frac{1}{2} + y, z$.

3. Discussion

3.1. Structures of simple acetoacetanilides

As suggested by Jeffrey (1997) the N—H···O=C hydrogen bonds of all compounds in this paper are characterized by presenting the N—H distance, the N—H···O distance, the N···O distance and the N—H···O angle. These data are given in Table 3 for each of the three crystal structures as well as for the structures already available in the literature. The N···O distance is seen to be short, in all cases it is below 3 Å, whilst in those molecules where an intramolecular hydrogen bond exists the N···O distance is around 2.7 Å.

As expected, each of the compounds (10), (11) and (12) adopts a *trans* planar configuration at the amide (Figs. 1, 2 and 3): however, the nature of the hydrogen bonding present then defines the orientation of the ketone carbonyl with respect to the amide. When intramolecular hydrogen bonding is present
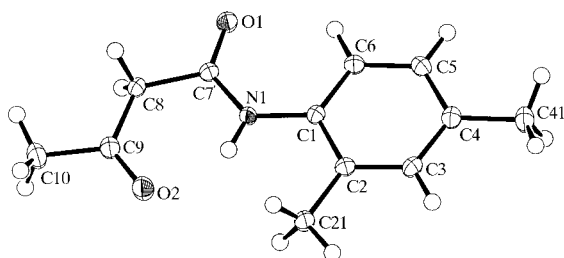
between the ketone carbonyl and the amide N—H, this serves to give a planar arrangement with a torsion angle between the two carbonyls of 176.2 (3)° in (12) and 180° in (10). Where an intermolecular hydrogen bond exists between the amide C=O and the amide N—H of a second molecule (Fig. 4), then the requirement to form a planar arrangement is lifted and the torsion angle in (11) is −70.3 (1)°. It should be noted that not only are the carbonyls co-planar in (10), but the entire molecule is flat with all non-H atoms on a crystal-lographic mirror plane. In (12) the plane of the aromatic ring and the amide plane are also nearly coplanar [the dihedral angle between these planes is 1.8 (1)°], whilst (11) shows a significant deviation from planarity in this region with a dihedral angle of 20.9 (1)°. These two trends of intramolecular hydrogen bonding being associated with both coplanar amide and ketone moieties and also coplanar amide and aromatic groups are also observed in those structures already found in the literature (see Table 4). It can be seen that the planar, intramolecularly hydrogen-bonded compounds all have an *ortho* ring substituent. It may be that the close proximity of the *ortho* substituent to the N—H group sterically disfavours intermolecular interactions and hence favours intramolecular hydrogen bonding. It is less obvious why *ortho* substitution favours coplanarity of the aromatic ring and the amide as the methyl substituents of (10) and (12) cannot form bifurcated hydrogen bonds, as is the case in the chloro derivative (6). That these *ortho* methyl groups are in close contact with the amide proton is supported by the lack of rotational motion observed in the crystal structures when compared to the *para* methyl groups of (10) and (11), which both show rotational disorder. This perhaps indicates that the *ortho* methyl groups are locked into place by interaction with the amide proton. Those compounds without an *ortho* substituent all favour intermolecular hydrogen-bond formation. This may be related to the geometry observed at C8: in those compounds with

Figure 1
*ORTEP*II (Johnson, 1976) view of acetoacet-*m*-xylidide (10) showing the atomic numbering scheme adopted for all compounds. Non-H atoms are shown as 50% probability ellipsoids and H atoms as spheres of arbitrary size.
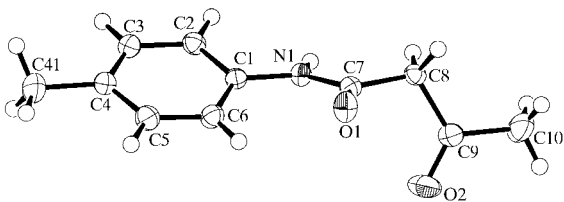

Figure 2
*ORTEP*II (Johnson, 1976) view of acetoacet-*p*-toluidide (11). Non-H atoms are shown as 50% probability ellipsoids and H atoms as spheres of arbitrary size.
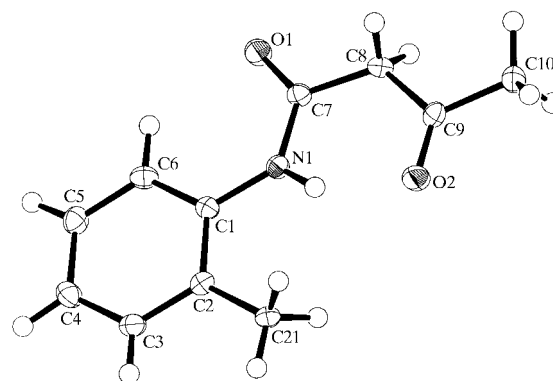

Figure 3
*ORTEP*II (Johnson, 1976) view of acetoacet-*o*-toluidide (12). Non-H atoms are shown as 50% probability ellipsoids and H atoms as spheres of arbitrary size.

Table 4
Torsion and dihedral angles (°).

Molecule	O=C···C=O torsion	Plane (aromatic ring/amide)	Hydrogen-bond type
Acetoacetanilide (1)	−64.3	33.7	Inter
Acetoaceto-o-chloroanilide (6)	−174.2	1.4	Intra
Acetoaceto-p-chloroanilide (7)	70.8	23.3	Inter
Acetoacet-p-anisidide (8)	−65.3	31.0	Inter
Azo pigment (9)	−177.8 (5)	8.6 (2)	Intra
Acetoacet-m-xylidide (10)	180	0	Intra
Acetoacet-p-toluidide (11)	−70.3 (1)	20.9 (1)	Inter
Acetoacet-o-toluidide (12)	176.2 (3)	1.8 (1)	Intra

Table 5
Selected bond distances (Å) and angles (°).

	(9)	(10)	(11)	(12)
C7—O1	1.254 (4)	1.225 (2)	1.227 (2)	1.225 (3)
C9—O2	1.221 (4)	1.216 (2)	1.212 (2)	1.222 (3)
C7—N1	1.342 (4)	1.354 (2)	1.352 (2)	1.361 (3)
C7—C8	1.490 (5)	1.526 (2)	1.509 (2)	1.520 (3)
C8—C9	1.502 (5)	1.508 (2)	1.511 (2)	1.514 (3)
C8—N2	1.304 (4)	–	–	–
N2—N3	1.331 (4)	–	–	–
C11—N3	1.392 (4)	–	–	–
C1—N1—C7	129.5 (3)	128.64 (13)	127.28 (12)	128.9 (2)
N1—C7—C8	115.7 (3)	116.11 (13)	115.06 (12)	116.2 (2)
C7—C8—C9	124.2 (3)	122.39 (13)	111.88 (12)	122.5 (2)
C8—C9—C10	118.7 (3)	115.63 (14)	115.81 (14)	115.5 (2)
C7—C8—N2	123.9 (3)	–	–	–
C9—C8—N2	111.9 (3)	–	–	–
C8—N2—N3	120.3 (3)	–	–	–
N2—N3—C11	117.6 (3)	–	–	–

intramolecular hydrogen bonds, the C7—C8—C9 angle is larger than would be expected for an sp^3 atom [122.4 (2) and 122.5 (2)° in (10) and (12), respectively]. The widening of this angle indicates the steric strain imposed upon these molecules by adopting their planar conformations. The non-planar species are not strained in this way and have normal tetrahedral geometries at C8 (see Table 5).

Molecule (10) forms anti-parallel stacks in the b direction held together by van der Waals forces: no specific interactions other than the intramolecular hydrogen bond can be identi-

fied. The structure of (12) is very similar to that of the m-xylidide derivative with no significant interactions present other than the intramolecular hydrogen bond. Molecule (11) has a more complex crystal structure. In addition to the amine intermolecular hydrogen bond, there is also a significant overlap between the methylene hydrogen H7 on C8 *syn* to the amide carbonyl and the ketone oxygen of an adjacent molecule [O2···H7(x, $-\frac{1}{2} - y, \frac{1}{2} + z$) = 2.34 (2) Å]. This results in the one-dimensional hydrogen-bonded chains becoming linked through this secondary hydrogen bond (Desiraju & Steiner, 1999) to give a two-dimensional sheet.
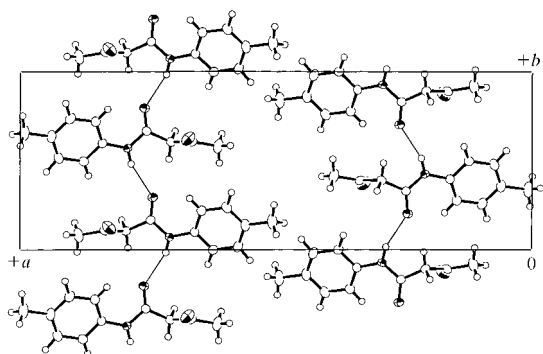
In order to determine the effect, if any, of this steric hindrance and the resultant change in hydrogen bonding we investigated the thermal properties of these compounds by differential scanning calorimetry. The melting points and heats of fusion are given in Table 6. In general, the effect of hydrogen bonding is less pronounced than expected and the dominating factor in most cases is the efficient overlap or close contact of the π–π orbitals of the aromatic rings and the carbonyl groups. For example, (12) has a well defined anti-parallel stack axis and close contact of the aromatic rings and the ketone carbonyl (C3···C9 = 3.56 Å), and has both a higher melting point and heat of fusion than its corresponding *para* isomer (11), where the molecules are inclined at an angle to each other. Similarly with acetoacetanilide (5) and acetoacet-m-xylidide (10), it is the xylidide which exhibits both greater overlap and has the higher melting point and heat of fusion. The structural relationship between these molecules is identical to that for (11) and (12) in that (5) exhibits molecules inclined at an angle to each other, whereas (10) shows anti-parallel stacking with close contacts between C1···C7 (3.32 Å) and C5···C9 (3.40 Å). An anomaly exists in the case of the chlorinated derivatives (6) and (7). In this case the trend is reversed with the *para* derivative exhibiting both the highest melting point and heat of fusion of all the samples. The hydrogen bond in (7) is not particularly strong (Table 3) and so this cannot provide an explanation. However, when
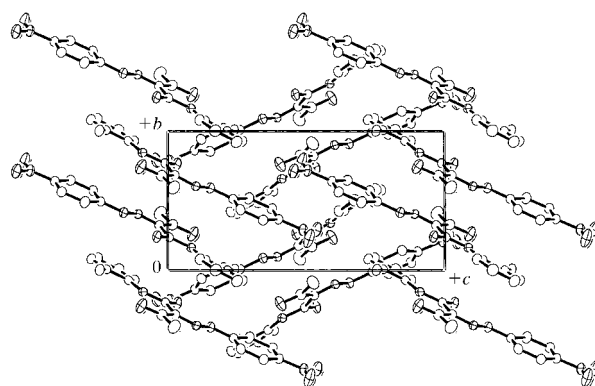

Figure 4
Packing diagram of acetoacet-p-toluidide (11) viewed along the c direction to illustrate the hydrogen-bonded chains.

Figure 5
Packing diagram of (9) viewed along the a direction.

Table 6
Thermal properties of acetoacetanilides.

Molecule	Melting point (K)	Heat of fusion (kJ mol^{-1})
Acetoacetanilide (1)	356.5	25.3
Acetoaceto-o-chloroanilide (6)	377	32.9
Acetoaceto-p-chloroanilide (7)	415	43.4
Acetoacet-p-anisidide (8)	387	28.2
Acetoacet-m-xylidide (10)	362	29.0
Acetoacet-p-toluidide (11)	366	24.3
Acetoacet-o-toluidide (12)	377	38.8

Table 7
Selected torsion angles (°).

	(9)	(10)	(11)	(12)
N1—C1—C2—C21	1.5 (5)	0	–	1.1 (3)
C7—N1—C1—C2	−176.1 (3)	180	157.9 (1)	178.5 (2)
C1—N1—C7—O1	2.0 (6)	0	3.0 (2)	0.3 (4)
C1—N1—C7—C8	−177.2 (3)	180	−176.1 (1)	−179.8 (2)
N1—C7—C8—C9	−0.2 (5)	0	−110.1 (1)	−2.0 (3)
O1—C7—C8—C9	−179.5 (3)	180	70.8 (2)	178.0 (2)
C7—C8—C9—O2	1.6 (6)	0	15.5 (2)	−0.8 (4)
N3—N2—C8—C7	−0.8 (5)	–	–	–
N3—N2—C8—C9	179.5 (3)	–	–	–
C8—N2—N3—C11	177.0 (3)	–	–	–
N2—N3—C11—C12	−173.7 (3)	–	–	–

Kubozono *et al.* (1992) first determined this crystal structure they noted a C—H···O=C interaction between a methylene proton and the amide carbonyl group. It is our belief that these interactions contribute to the stability of the *para*-chloro derivative.

3.2. Structure of *N*-(2-methyl)phenyl-2-(4-nitrophenylhydrazono)-3-oxobutyramide (9)

The pigment (9) was prepared in the straightforward manner given in the scheme above. The periodic structure of (9) is given in Fig. 5. The principal feature of this structure is the molecular stacks extending in the direction of the *b* axis. In the *c* direction these stacks are parallel and in the *a* direction form a herringbone arrangement. In common with other pigments of this structural type it does not exist as the azo tautomer, but instead adopts the keto-hydrazo form as shown by the long N—N distance [1.331 (4) Å compared to *ca* 1.250 Å for genuine azo compounds (Crispini *et al.*, 1998)] and by the short N2—C8 distance of 1.304 (4) Å. In addition, the interatomic distances N1···O2 and N3···O1 of 2.661 (4) and 2.573 (4) Å, respectively, suggest intramolecular hydrogen
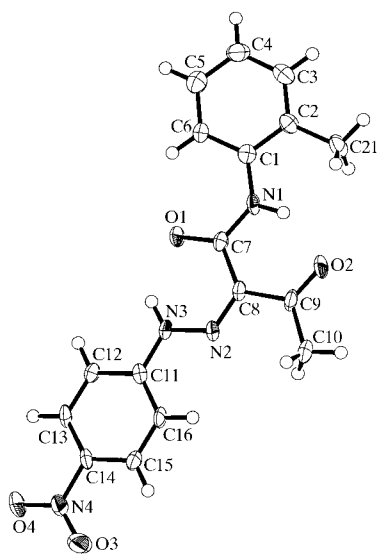

Figure 6
*ORTEP*II (Johnson, 1976) view of (9) showing the atomic numbering scheme. Non-H atoms are shown as 50% probability ellipsoids and H atoms as spheres of arbitrary size.

bonds. These hydrogen bonds cause the molecule to adopt a planar conformation about the amide fragment (see torsion angles, Table 7). Thus, the structure of (9) (Fig. 6) follows the pattern set by the simple acetoacetanilides in that it is *ortho* substituted and thus has internal hydrogen bonding which gives a planar conformation. However, reviewing the work of previous authors (Paulus *et al.*, 1983; Paulus, 1984; Gridunova *et al.*, 1991; Paulus & Rieper, 1985; Whitaker, 1983*a*,*b*, 1984*a*,*b*, 1985*a*,*b*,*c*, 1986, 1987; Whitaker & Walker, 1987; Golinski, 1988) has shown us that for those anilides which show an intermolecular hydrogen bond, this is not necessarily retained in the simple monoazo pigments derived from these compounds and that in all cases, irrespective of the nature of any aryl ring substituents, the pigments show intramolecular hydrogen bonding similar to that found in (9). Furthermore, there appears to be no correlation between the aryl ring substituents and the dihedral angle between the ring plane and the plane of the amide. In the simple acetoacetanilides we suggested that intramolecular hydrogen bonding was disfavoured by the need to open the angle subtended by C8 from a tetrahedral value to *ca* 122° and hence only occurred when intermolecular interactions were blocked by *ortho* substituents. This is not the case for azo pigments derived from acetoacetanilides as C8 is an *sp*² hybridized atom.

If one compares the structure of (9) with that of its parent molecule (12), then several differences can be observed. The N1···O2 distance in the hydrogen bond is shortened [2.661 (4) Å for (9), *ca* 2.704 (3) Å for (12) and a range of 2.633–2.684 Å for those pigments found in the Cambridge Structural Database (Allen & Kennard, 1993)], as is the corresponding N—H···O distance. This is presumably due to a combination of the additional π–π system α to the ketone in (9) as well as additional geometrical constraints imposed on the molecule due to the other six-membered hydrogen-bonded system present in the pigment. From Table 4 it can be seen that the torsion angles between the carbonyl groups are similar in magnitude, but in (9) the sign has switched to −177.8 (5)°. Finally, the angle between the plane of the anilide aromatic ring and the amide is now 8.6 (2)°, representing a significant deviation from planarity in (9).

The structures of the acetoacetanilides presented here highlight the differences in hydrogen-bonding networks which

can be engineered by a simple change in the position of a substituent. That such profound effects on intermolecular hydrogen bonding can be achieved by simple changes in structure underlines the importance of considering the periodic structure of a molecule in concert with molecular structure when designing new molecular crystals. Furthermore, we have demonstrated that it is not always possible to extrapolate the periodic structure of a structural fragment to that of the final product even in a relatively simple case such as that described here.

References

Alcock, N. W., Spencer, R. C., Prince, R. H. & Kennard, O. (1968). *J. Chem. Soc. A*, pp. 2383–2388.

Allen, F. H. & Kennard, O. (1993). *Chem. Des. Autom. News*, **8**, 31.

Anderson, S., Clegg, W. & Anderson, H. L. (1998). *Chem. Commun.* pp. 2379–2380.

Bertolasi, V., Gilli, P., Ferretti, V. & Gilli, G. (1995). *Acta Cryst.* B**51**, 1004–1015.

Cernik, R. J., Clegg, W., Catlow, C. R. A., Bushnell Wye, G., Flaherty, J. V., Greaves, G. W., Burrows, I., Taylor, D. J., Teat, S. J. & Hamichi, M. (1997). *J. Synchrotron Rad.* **4**, 279–286.

Clegg, W., Elsegood, M. R. J., Teat, S. J., Redshaw, C. & Gibson, V. C. (1998). *J. Chem. Soc. Dalton Trans.* pp. 3037–3039.

Crispini, A., Ghedini, M. & Pucci, D. (1998). *Acta Cryst.* C**54**, 1869–1871.

Desiraju, G. R. & Steiner, T. (1999). *The Weak Hydrogen Bond in Structural Chemistry and Biology.* Open University Press, New York.

Diamantis, A. A., Manikas, M., Salam, M. A. & Tiekink, E. R. T. (1992). *Z. Kristallogr.* **202**, 154–156.

Golinski, B. (1988). *Z. Kristallogr.* **184**, 161–167.

Grainger, C. T. & McConnell, J. F. (1969). *Acta Cryst.* B**25**, 1962–1970.

Gridunova, G. V., Tafeenko, V. A., Tambieva, O. A., Lisitsyna, E. S. & Medev, S. V. (1991). *Zh. Strukt. Khim.* **32**, 358–361.

Guggenberger, L. J. & Teufer, G. (1975). *Acta Cryst.* B**31**, 785–790.

Hao, Z. & Iqbal, A. (1997). *Chem. Soc. Rev.* **26**, 203–213.

Jarvis, J. A. J. (1961). *Acta Cryst.* **14**, 961–964.

Jeffrey, G. A. (1997). *An Introduction to Hydrogen Bonding.* Oxford University Press.

Johnson, C. K. (1976). *ORTEP*II. Report ORNL-5138. Oak Ridge National Laboratory, Tennessee, USA.

Kennedy, A. R., McNair, C., Smith, W. E., Chisholm, G. & Teat, S. J. (2000). *Angew. Chem. Int. Ed.* **39**, 638–640.

Kobelt, D., Paulus, E. F. & Kunstmann, W. (1972). *Acta Cryst.* B**28**, 1319–1324.

Kobelt, D., Paulus, E. F. & Kunstmann, W. (1974). *Z. Kristallogr.* **139**, 15–32.

Kubozono, Y., Kohno, I., Ooishi, K., Namazue, S., Haisa, M. & Kashino, S. (1992). *Bull. Chem. Soc. Jpn*, **65**, 3234–3240.

Molecular Structure Corporation (1985). *MSC/AFC Diffractometer Control Software.* MSC, 3200 Research Forest Drive, The Woodlands, TX 77381, USA.

Molecular Structure Corporation (1993). *TEXSAN. Single Crystal Structure Analysis Package.* Version 1.6. MSC, 3200 Research Forest Drive, The Woodlands, TX 77381, USA.

Olivieri, A. C., Wilson, R. B., Paul, I. C. & Curtin, D. Y. (1989). *J. Am. Chem. Soc.* **111**, 5525–5532.

Paulus, E. F. (1984). *Z. Kristallogr.* **167**, 65–72.

Paulus, E. F. & Rieper, W. (1985). *Z. Kristallogr.* **171**, 87–100.

Paulus, E. F., Rieper, W. & Wagner, D. (1983). *Z. Kristallogr.* **165**, 137–149.

Salmen, R., Malterud, K. E. & Pedersen, B. F. (1988). *Acta Chem. Scand. A*, **42**, 493–499.

Sheldrick, G. M. (1990). *SHELXS.* University of Göttingen, Germany.

Sheldrick, G. M. (1997). *SHELXL*97. University of Göttingen, Germany.

Siemens (1995). *SMART.* Siemens Analytical X-ray Instruments Inc., Madison, Wisconsin, USA.

Whitaker, A. (1977). *Z. Kristallogr.* **145**, 271–288.

Whitaker, A. (1978*a*). *Z. Kristallogr.* **146**, 173–184.

Whitaker A. (1978*b*). *Z. Kristallogr.* **147**, 99–112.

Whitaker, A. (1983*a*). *Z. Kristallogr.* **163**, 19–30.

Whitaker, A. (1983*b*). *Z. Kristallogr.* **163**, 139–149.

Whitaker, A. (1984*a*). *Z. Kristallogr.* **166**, 177–188.

Whitaker, A. (1984*b*). *Z. Kristallogr.* **167**, 225–233.

Whitaker, A. (1985*a*). *Z. Kristallogr.* **170**, 213–223.

Whitaker, A. (1985*b*). *Z. Kristallogr.* **171**, 7–15.

Whitaker, A. (1985*c*). *Z. Kristallogr.* **171**, 17–22.

Whitaker, A. (1986). *Acta Cryst.* C**42**, 1566–1569.

Whitaker, A. (1987). *Acta Cryst.* C**43**, 2141–2144.

Whitaker, A. & Walker, N. P. C. (1987). *Acta Cryst.* C**43**, 2137–2141.